Transactions, **SMiRT-26**
Berlin/Potsdam, Germany, July 10-15, 2022
Division V

SEISMIC ENERGY FLOW AND BALANCE IN EARTHQUAKE SOIL STRUCTURE INTERACTION SYSTEMS

Han Yang[1], Hexiang Wang[2], Boris Jeremić[3]

[1] Postdoctoral Researcher, University of California, Davis, CA, USA
[2] Engineer, Berkshire Hathaway Specialty Insurance, San Ramon, CA, USA
[3] Professor, University of California, Davis, CA, USA (jeremic@ucdavis.edu)

ABSTRACT

Presented is a methodology to accurately account for all input and dissipated mechanical energy in a soil structure interaction (SSI) system during seismic excitations. Developed methodology is based on recent work on analysis of energy dissipation in solids and structures Yang et al. (2018, 2019a,c,b). Input seismic energy is comprised of incoming seismic waves. Multiple mechanisms of energy dissipation are present in a SSI system. Proper calculations of energy input and energy dissipation due to various mechanisms are presented. The importance of incorporation of plastic free energy, that ensures nonnegative incremental energy dissipation, also known as the second law of thermodynamics, is emphasized. Energy input and dissipation analysis is illustrated using a numerical example of SSI system under seismic excitation. Practical uses of energy analysis for SSI systems, or energy-based design concepts, are also discussed. Energy input and dissipation calculation methods are implemented and available within the Real-ESSI Simulator system (Jeremić et al., 2022a), `http://real-essi.us/`.

INTRODUCTION

The use of energy dissipation, as well as other energy-based parameters, is gaining popularity in design of structures and soil structure interaction (SSI) systems. Papazafeiropoulos et al. (2017) pointed out that force-based and displacement-based design concepts mainly focus on the peak responses, while the loading history is properly considered. During a seismic event, SSI systems are continuously shaked, deformed, and potentially damaged throughout the loading history. This can only be captured by energy parameters, such as energy input and plastic energy dissipation. Therefore, it is advantageous to use energy analysis in evaluation of seismic resiliency of SSI systems, including nuclear installations (NIs).

Due to the limit of computational power and a lacking in complex modeling techniques, early energy-based design (EBD) concepts are relatively simplified (Zahrah and Hall, 1982, Uang and Bertero, 1990, Sucuoğlu and Nurtuğ, 1995, Trifunac et al., 2001). Many recent studies were developed upon the early EBD concepts and incorporates more practical considerations (Manfredi, 2001, Moustafa, 2011, Mezgebo and Lui, 2017, Papazafeiropoulos et al., 2017). It should be pointed out that EBD approaches have been fairly successful, and continue to evolve and gain popularity. The Real-ESSI Simulator (Jeremić et al., 2022a) used in this study is a high fidelity numerical tool that is capable of modeling the nonlinear, inelastic behavior of SSI system.

Figure 1 illustrates processes and mechanisms of the propagation and dissipation of seismic energy, from earthquake source to location of the soil structure system. Before reaching the site, part of the seismic

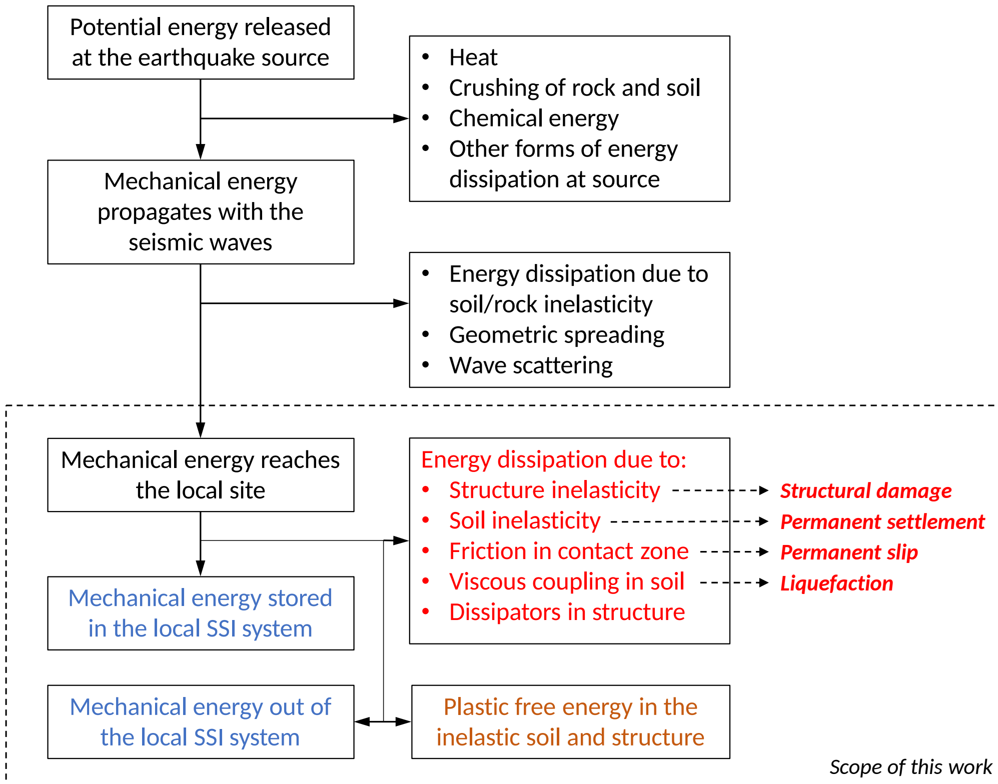

Figure 1: Seismic energy propagation and dissipation, from source to local site.

energy is reflected back and propagates outside of the local domain of interest, known as radiation damping. Upon reaching the site, the rest of the mechanical energy carried by the seismic waves flows through the local SSI system, and leads to the dynamic responses of soil and structure.

There are a number of potential dissipation mechanisms, physical and mathematical/algorithmic, in the modeling of SSI system:

- wave reflections
- radiation damping
- viscous coupling with internal, pore fluids
- viscous coupling with external fluids, in tanks, pools, etc.
- inelastic behavior of soil and rock
- inelastic behavior of concrete and steel
- inelastic behavior of interfaces, contacts and joints
- inelastic behavior of energy dissipator devices
- numerical, algorithmic energy dissipation and production (!)

One major challenge seen in previous studies is the proper identification of all energy terms and energy dissipation mechanisms. Particularly, the omission of plastic free energy has been observed in most analysis methods, as well as a large number of publications. This omission not only directly violates the second law of thermodynamics but also leads to inaccurate/unreliable energy analysis results.

The theoretical and computational basis for each energy dissipation mechanism was laid out in a series of publications Yang et al. (2018, 2019a,b,c). Presented here is an integrated EBD framework that incorporates all previously developed methods. During any significant seismic event, majority of energy should be designed to dissipate through inelasticity of soil and contact zone, while energy dissipators (frictional pendulum, etc.) can also be used for such purposes. Design of new and upgrade of current NIs can benefit from presented methodology. For example, new design and upgrade of current NIs can be modified to dissipate seismic energy in soil, contact zone, and dissipation devices, and away from structural components.

THEORETICAL FRAMEWORK

Within a SSI system, seismic energy is dissipated due to material inelasticity (in soil, structure, and contact zone), viscous coupling between soil grains and pore fluids, and energy dissipators placed in the building or foundation. On top of the physical dissipative processes, algorithmic damping is frequently used to achieve stable simulation result in numerical studies. These energy dissipation mechanisms model fundamentally different physical or mathematical phenomena, and lead to different system responses. It is important to model each energy dissipation mechanism by following proper physics and mathematics. The presented framework focuses on modeling the transformation and dissipation of seismic energy after it reaches a local SSI system.

According to Yang et al. (2019c), the incremental form of energy balance for a dynamic inelastic system can be expressed as

$$\Delta W_{Input} = \Delta E_K + \Delta D_V + \Delta E_S + \Delta E_P + \Delta D_P \tag{1}$$

where the right hand side of Equation 1 is the increment of external input work ΔW_{Input}, the five terms on the left hand side of Equation 1 are the incremental kinetic energy ΔE_K, the incremental viscous energy dissipation ΔD_V, the incremental elastic strain energy ΔE_S, the incremental plastic free energy ΔE_P, and the incremental plastic energy dissipation ΔD_P.

Note that, for different inelastic material models, the calculations of energy dissipation have different forms. The energy calculation approaches for various material models and energy dissipation mechanisms were derived in previous studies by Yang et al. (2018, 2019a,b,c). Two key components of the presented EBD framework are presented below.

Hyperbolic Drucker-Prager Plasticity for Pressure-Dependent Solid

Drucker-Prager type plasticity is used to model pressure-dependent materials, like soils and rocks. Collins and Houlsby (1997) and Yang et al. (2019b) pointed out that non-associated plastic flow rule should be used for pressure-dependent frictional material. Thus, the Drucker-Prager plasticity referred to in this paper is non-associated, which means that the plastic flow direction is not necessarily normal to the yield surface. In order to improve the plasticity model's performance and stability in low-confinment conditions, a hyperbolic modification to the classic Drucker-Prager model is applied and presented below. More details on this consitutive model can be found in Jeremić et al. (2022b).

Hyperbolic Drucker–Prager Yield Function The hyperbolic Drucker-Prager yield function considering isotropic and kinematic hardening is given as

$$f = \sqrt{(s_{ij} - p\alpha_{ij})(s_{ij} - p\alpha_{ij}) + \frac{2}{3}k^2a^2} - \sqrt{\frac{2}{3}}kp - \sqrt{2}\beta \tag{2}$$

where s_{ij} is the deviatoric stress tensor, p is the isotropic mean pressure, α_{ij} is the back-stress ratio tensor, k is a constitutive surface parameter, a is the rounded distance related to the yield surface's hyperbolic shape,

$$\beta = \frac{6\cos\phi_0}{\sqrt{3}(3-\sin\phi_0)}c \tag{3}$$

, ϕ_0 is the initial friction angle and c is the cohesion.

Plastic Flow The non-associated plastic flow is defined as

$$m_{ij} = \left(\frac{\partial f}{\partial \sigma_{ij}}\right)^{dev} - \frac{1}{3}D\delta_{ij} = \left(s_{ij} - p\alpha_{ij}\right)\left[\left(s_{rs} - p\alpha_{rs}\right)\left(s_{rs} - p\alpha_{rs}\right) + \frac{2}{3}k^2a^2\right]^{-0.5} - \frac{1}{3}D\delta_{ij} \tag{4}$$

where

$$D = \xi\left(\sqrt{\frac{2}{3}}k_d - \frac{\sqrt{s_{mn}s_{mn}}}{p}\right) \tag{5}$$

, ξ and k_d are material parameters that control the contractive/dilative behavior of the model.

Linear Isotropic Hardening Linear isotropic hardening is used for this material model. The evolution of the internal variable k is defined as

$$\bar{k} = Hm^{equi} \quad , \quad m^{equi} = \left(\frac{2}{3}m_{ij}m_{ij}\right)^{0.5} \tag{6}$$

where H is a material constant.

Armstrong-Frederick kinematic hardening for Hyperbolic Drucker-Prager

$$\bar{\alpha}_{ij} = \frac{2}{3}\frac{h_a}{p_{atm}}m_{ij}^{dev} - c_r\left(\frac{2}{3}m_{rs}^{dev}m_{rs}^{dev}\right)^{0.5}\alpha_{ij} \tag{7}$$

where p_{atm} is the atmospheric pressure of 101.325 kPa. The unit of parameter h_a is Pascal. The parameter c_r is unitless. The α_{ij} in Drucker-Prager is unitless.

Energy Calculation For non-associated Drucker-Prager plasticity model with Armstrong-Frederick kinematic hardening, the incremental plastic free energy density is written as

$$\Delta\psi^{pl} = \left(\frac{3}{2h_a}\alpha_{ij}\Delta\alpha_{ij} - m_{ii}^{vol}\Delta\lambda\right)p \tag{8}$$

where m_{ij}^{vol} is the volumetric part of the normalized plastic flow direction tensor m_{ij}, $\Delta\lambda$ is the scalar loading index that equals to the magnitude of incremental plastic strain.

The incremental plastic energy dissipation density is written as

$$\Phi = \sigma_{ij}\Delta\epsilon_{ij} - \sigma_{ij}\Delta\epsilon_{ij}^{el} - \Delta\Psi^{pl} = \sigma_{ij}\Delta\epsilon_{ij}^{pl} - \Delta\Psi^{pl} \geq 0 \tag{9}$$

where Φ is the incremental plastic energy dissipation density, σ_{ij} is the stress tensor, $\Delta\epsilon_{ij}$ is the incremental strain tensor, $\Delta\epsilon_{ij}^{el}$ is the incremental elastic strain tensor, $\Delta\epsilon_{ij}^{pl}$ is the incremental plastic strain tensor, and

$\Delta\Psi^{pl}$ is the incremental plastic free energy density. It is worth pointing out that, according to the second law of thermodynamics, the incremental plastic energy dissipation density should always be nonnegative during any time period. The violations of this law were observed in a large number of published papers, and continues to emerge in more recent publications.

Soil-Foundation Interface Material

The soil-foundation interface is a thin layer of soil that is adjacent to the foundation. Significant seismic energy often dissipates within the interface zone before reaching the structure. It is necessary to include the modeling of energy dissipation for soil-structure interface zone within the energy analysis framework. The interface material model used in this study was developed by Sinha and Jeremić (2017). The stress-based interface model is capable of modeling the normal, axial nonlinear response when the gap is closed. Normal, axial response also allows for gap to open, through material nonlinear response. Shear, tangential behavior is modeled using frictional slip, with a a number of different material models controlling such inelastic shear behavior.

Normal Behavior As note above, the normal behavior is nonlinear elastic with no tensile capacity. The normal stress σ_n and normal stiffness k_n are defined as

$$\sigma_n = k_i e^{-S_r \epsilon} \epsilon \tag{10}$$

$$k_n = k_i e^{-S_r \epsilon}(1 - S_r \epsilon) \tag{11}$$

where k_i is the initial normal stiffness between soil-structure interface, S_r is the stiffening rate, and ϵ is the penetration or normal strain. Note that a maximum normal stiffness k_n^{max} is applied as a limiting case in order to avoid numerical instability.

Shear Behavior The shear component of the interface model follows the elastoplastic theory. In order to make the interface shear behavior pressure-dependent, the elastic shear stiffness k_t is related to the normal stress σ_n. For a given normal stress σ_n, the shear stiffness k_t is defined as

$$k_t = k_{t0} \frac{\sigma_n}{\sigma_{p0}} \tag{12}$$

where σ_{p0} is the constant reference stress of 101.3kPa and k_{t0} is the shear stiffness at the reference normal stress. The yielding, slipping condition is determined by the following yield function

$$f = \left(\frac{\tau_1}{\sigma_n} - \alpha_1 \right)^2 + \left(\frac{\tau_2}{\sigma_n} - \alpha_2 \right)^2 = 0 \tag{13}$$

where τ_1 and τ_2 are the shear stress components and α_1 and α_2 are the corresponding back stress components. The evolution of back stress is of a nonlinear Armstrong-Frederick hardening type that is given as

$$\Delta\alpha_1 = k_t \Delta\gamma_1^p - \frac{k_t}{\mu_r} |\Delta\gamma^p| \alpha_1 \tag{14}$$

$$\Delta\alpha_2 = k_t \Delta\gamma_2^p - \frac{k_t}{\mu_r} |\Delta\gamma^p| \alpha_2 \tag{15}$$

where γ_1^p, γ_2^p are the plastic parts of the shear strains, μ_r is the residual, or peak normalized shear stress, and $|\Delta\gamma^p|$ is the magnitude of the incremental plastic strain defined as $|\Delta\gamma^p| = \sqrt{\Delta\gamma_1^p \Delta\gamma_2^p}$.

Energy Calculation The energy calculation for the interface material was presented by Sinha and Jeremić (2017) based on the work by Yang et al. (2018). Since the normal behavior of the material model is nonlinear elastic, the plastic energy dissipation results from the frictional slipping in the shear directions. The incremental plastic free energy density is given as

$$\Delta\Psi^{pl} = \frac{1}{k_t}(\alpha_1 \Delta\alpha_1 + \alpha_2 \Delta\alpha_2) \tag{16}$$

The incremental plastic energy dissipation is then calculated from

$$\Phi = (\tau_1 \Delta\gamma_1^p + \tau_2 \Delta\gamma_2^p) - \Delta\Psi^{pl} \tag{17}$$

NUMERICAL EXAMPLE

Model Description

An overview of the SSI model is shown in Figure 2. The main components of the model are:

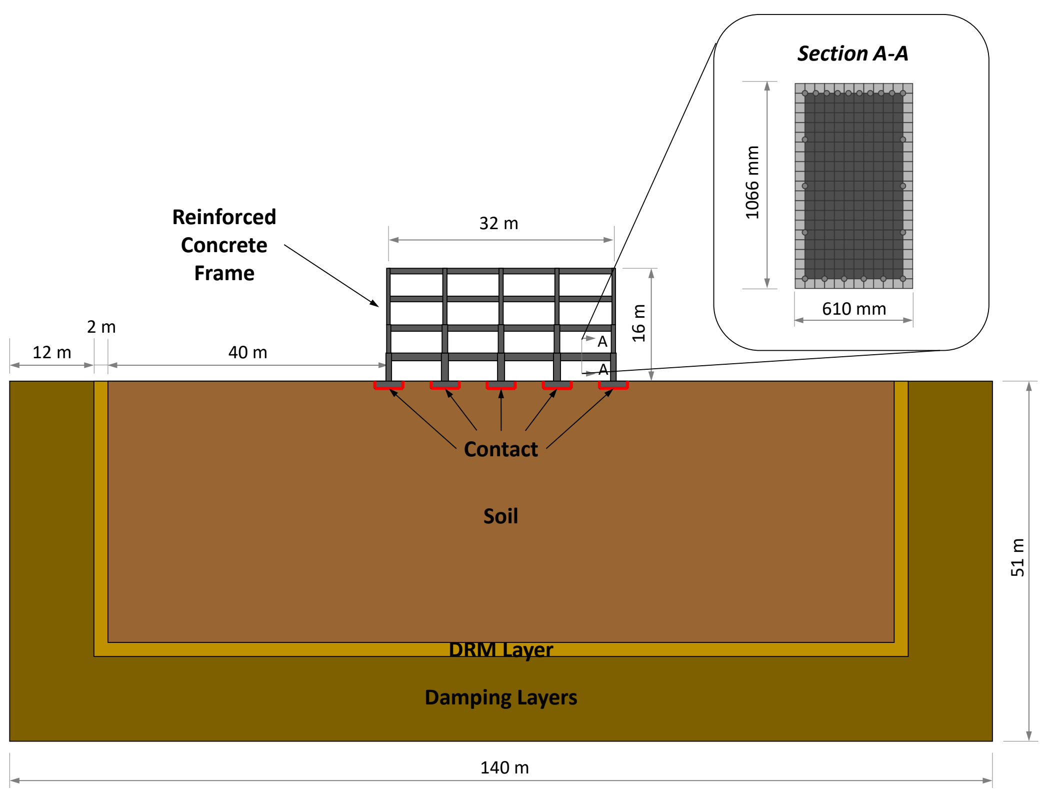

Figure 2: Numerical model of the reinforced concrete frame, inelastic soil, and frictional interfaces.

- A reinforced concrete frame that is modeled using beam-column elements, that are developed using previously discussed steel and concrete fiber material models. Frame model is constrained to the loading plane, it is a 2D frame model. The four story, four bay frame is based on one of the code-conforming designs by Haselton et al. (2008).
- The underlying soil that is modeled using standard 27-node-brick elements constrained to deform in the loading plane.
- The underlying soil is modeled using the hyperbolic Drucker-Prager model with Armstrong-Frederick kinematic hardening.
- The interfaces between soil and foundation is modeled using the nonlinear, stress-based, frictional slipping contact/interface elements.
- A layer of Domain Reduction Method (DRM) elements, for applying seismic excitations (Bielak et al., 2003), is modeled using 27-node-brick elements and linear elastic material.
- A few damping layers outside of the DRM layer, to absorb the very small outgoing waves, representing radiation damping from oscillations of the structure, are used, with progressively increasing Rayleigh damping.

Energy Analysis Results

Figure 3 shows the distribution of plastic energy dissipation density evolving with time. Note that for

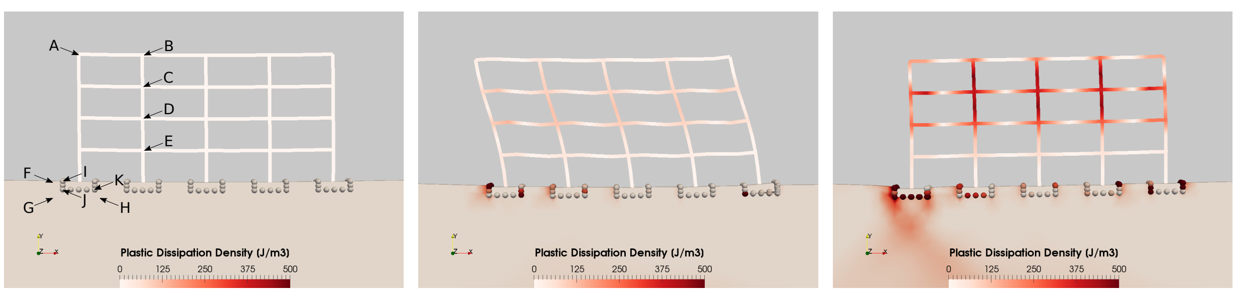

(a) t = 5 s (b) t = 6 s (c) t = 8 s

Figure 3: Distribution of plastic energy dissipation density evolving with time.

interface elements between foundation and soil, with very small volume, small spheres are used to represent those elements in energy dissipation visualization. At time $t = 5$s, as shown in Figure 3(a), before any significant seismic motion excites the frame, there is no plastic dissipation in the model. After that, between time $t = 5$s and time $t = 8$s, plastic dissipation continuously accumulates within the frame, underlying soil, and soil-structure interface zone.

Figure 3, shows that plastic dissipation in frame elements is concentrated around the connections between beams and columns. Significant plastic dissipation is accumulated in the top two floors, while the lower floors experience almost no dissipation. Plastic dissipation in surface soil is mainly concentrated near the foundations. Large amount of plastic dissipation is observed near the left footing. Another interesting observation is that the damage zone in soil penetrates to some depth. This indicates not only large localized deformation around footing, but also significant settlement accumulated throughout the soil layer.

CONCLUSION

Presented was an improved EBD analysis framework developed based on proper thermodynamics and mechanics for SSI systems, including NIs. Theoretical equations for energy dissipation due to various mechanisms were presented and discussed. The calculation of plastic energy dissipation should properly consider all forms of energy in inelastic materials, especially plastic free energy. It was also noted that each energy dissipation mechanism should be modeled individually and properly, to ensure the reliability of numerical simulation results.

A practical SSI example was used to illustrate the developed methodology. Inelastic, pressure-dependent hyperbolic Drucker-Prager material model was used for soil. Frictional slipping interface between soil and foundation was also modeled using contact elements. Input seismic motion was applied using DRM with absorbing boundary layers. Significant plastic dissipation was observed in various locations of the SSI model. The accumulation of plastic dissipation throughout the loading history was also discussed. Using these energy analysis results, the safety of SSI system designs can be evaluated and improved.

ACKNOWLEDGMENT

This work was partially supported by the US-DOE.

REFERENCES

Bielak, J., Loukakis, K., Hisada, Y., and Yoshimura, C. (2003). “Domain reduction method for three–dimensional earthquake modeling in localized regions. part I: Theory.” *Bulletin of the Seismological Society of America*, 93(2), 817–824.

Collins, I. F. and Houlsby, G. T. (1997). “Application of thermomechanical principles to the modelling of geotechnical materials.” *Procedings of Royal Society London*, 453, 1975–2001.

Haselton, C. B., Goulet, C. A., Mitrani-Reiser, J., Beck, J. L., Deierlein, G. G., Porter, K. A., Stewart, J. P., and Taciroglu, E. (2008). “An assessment to benchmark the seismic performance of a code-conforming reinforced-concrete moment-frame building.” *Report No. 2007/1*, Pacific Earthquake Engineering Research Center.

Jeremić, B., Jie, G., Cheng, Z., Tafazzoli, N., Tasiopoulou, P., Pisanò, F., Abell, J. A., Watanabe, K., Feng, Y., Sinha, S. K., Behbehani, F., Yang, H., and Wang, H. (1988-2022a). *The Real-ESSI Simulator System*. University of California, Davis. `http://real-essi.us/`.

Jeremić, B., Yang, Z., Cheng, Z., Jie, G., Tafazzoli, N., Preisig, M., Tasiopoulou, P., Pisanò, F., Abell, J., Watanabe, K., Feng, Y., Sinha, S. K., Behbehani, F., Yang, H., and Wang, H. (1989-2022b). *Nonlinear Finite Elements: Modeling and Simulation of Earthquakes, Soils, Structures and their Interaction*. University of California, Davis, CA, USA URL: `http://sokocalo.engr.ucdavis.edu/~jeremic/LectureNotes/`.

Manfredi, G. (2001). “Evaluation of seismic energy demand.” *Earthquake Engineering & Structural Dynamics*, 30(4), 485–499.

Mezgebo, M. G. and Lui, E. M. (2017). “A new methodology for energy-based seismic design of steel moment frames.” *Earthquake Engineering and Engineering Vibration*, 16(1), 131–152.

Moustafa, A. (2011). “Damage-based design earthquake loads for single-degree-of-freedom inelastic structures.” *Journal of Structural Engineering*, 137(3), 456–467.

Papazafeiropoulos, G., Plevris, V., and Papadrakakis, M. (2017). “A new energy-based structural design optimization concept under seismic actions.” *Frontiers in Built Environment*, 3, 44.

Sinha, S. K. and Jeremić, B. (2017). "Modeling of dry and saturated soil-foundation contact." *Report No. UCD–CompGeoMech–01–2017*, University of California, Davis (August).

Sucuoğlu, H. and Nurtuğ, A. (1995). "Earthquake ground motion characteristics and seismic energy dissipation." *Earthquake Engineering & Structural Dynamics*, 24(9), 1195–1213.

Trifunac, M. D., Ying Hao, T., and Todorovska, M. I. (2001). "Energy of earthquake as a design tool." *Proceedings of 13th Mexican Conference on Earthquake Engineering, XIII MCEE*, Guadalajara, Mexico, 1–49 (31th October – 3rd November).

Uang, C.-M. and Bertero, V. V. (1990). "Evaluation of seismic energy in structures." *Earthquake Engineering & Structural Dynamics*, 19(1), 77–90.

Yang, H., Feng, Y., Wang, H., and Jeremić, B. (2019a). "Energy dissipation analysis for inelastic reinforced concrete and steel beam-columns." *Engineering Structures*, 197, 109431.

Yang, H., Sinha, S. K., Feng, Y., McCallen, D. B., and Jeremić, B. (2018). "Energy dissipation analysis of elastic-plastic materials." *Computer Methods in Applied Mechanics and Engineering*, 331, 309–326.

Yang, H., Wang, H., Feng, Y., and Jeremić, B. (2019b). "Plastic energy dissipation in pressure-dependent materials." *ASCE Journal of Engineering Mechanics* In Print.

Yang, H., Wang, H., Feng, Y., Wang, F., and Jeremić, B. (2019c). "Energy dissipation in solids due to material inelasticity, viscous coupling, and algorithmic damping." *ASCE Journal of Engineering Mechanics*, 145(9).

Zahrah, T. F. and Hall, W. J. (1982). "Seismic energy absorption in simple structures." *Report no.*, University of Illinois Engineering Experiment Station.